Absolute and Site-Specific Abstraction Rate Coefficients for Reactions of Cl with CH_3CH_2OH, CH_3CD_2OH, and CD_3CH_2OH between 295 and 600 K

Craig A. Taatjes*

Combustion Research Facility, Mail Stop 9055, Sandia National Laboratories, Livermore, California 94551-0969

Lene K. Christensen, Michael D. Hurley, and Timothy J. Wallington*

Research Staff, Ford Motor Company, SRL-3083, Dearborn, Michigan 48121-2053

Received: July 20, 1999; In Final Form: October 5, 1999

Absolute rate coefficients for reactions of Cl atoms with selectively deuterated ethanols have been measured between 295 and 600 K by a laser-photolysis/CW infrared absorption method. Yields of HCl are determined by comparison with the Cl + ethane or Cl + propane reaction, permitting site-specific branching fractions to be derived. Smog chamber experiments with Fourier transform infrared (FTIR) detection are performed to determine products of the room-temperature Cl + C_2H_5OH reaction. The rate coefficients for all ethanols display only a slight temperature dependence and can be parametrized by simple Arrhenius expressions: $k_{CH_3CH_2OH} = (9.4 \pm 1.4) \times 10^{-11}e^{(45 \pm 32)/T}$, $k_{CD_3CH_2OH} = (6.6 \pm 0.9) \times 10^{-11}e^{(90 \pm 40)/T}$, and $k_{CH_3CD_2OH} = (6.9 \pm 0.7) \times 10^{-11}e^{(-76 \pm 40)/T}$ cm^3 molecule^{-1} s^{-1} (error bars $\pm 2\sigma$). Combining the results from the present work with literature data, we recommend $k_{CH_3CH_2OH} = (9.5 \pm 1.9) \times 10^{-11}$ cm^3 molecule^{-1} s^{-1} at 298 K. The room-temperature contribution of abstraction at the methyl site is found to be 0.07 ± 0.02 from FTIR product analysis of the Cl + CH_3CH_2OH reaction and 0.08 ± 0.02 from laser photolysis/CW infrared absorption measurements (error bars $\pm 2\sigma$). Abstraction of the hydroxyl hydrogen is negligible. A small but significant amount of HCl ($v = 1$) is produced in the Cl + CD_3CH_2OH and Cl + CH_3CH_2OH reactions at room temperature.

Introduction

The reactions of Cl atoms with organic species (predominantly methane) are important removal mechanisms for Cl in the stratosphere and act in the oxidation of organic species in the troposphere. The atmospheric importance of chlorine reactions has fueled interest in more general aspects of Cl atom reactivity. In addition, since C−H and Cl−H bond energies are similar, hydrogen abstraction reactions of Cl atoms are commonly used as selective sources of radical species in laboratory kinetic studies. The reactions of Cl with alcohols in particular has been exploited to form selected hydroxyalkyl radicals. The utility of such a preparation scheme depends on an understanding of the site selectivity of the Cl atom reaction.

Chlorine atoms are known to react rapidly with alcohols by abstracting a hydrogen from the alkyl group. The reaction with methanol has been studied extensively, and the rate coefficient is relatively well-established over a wide temperature range. Discharge-flow studies have determined that the Cl + CH_3OH reaction forms exclusively CH_2OH.[1,2] The reactions with higher alcohols have attracted less study. Relative-rate measurements have been reported for Cl + ethanol and propanols at room temperature,[3−6] but no absolute rate coefficient measurements or temperature-dependent measurements have been reported. Mass spectroscopic investigations have indicated a strong preference for formation of secondary hydroxyalkyl radicals in Cl + alcohol reactions,[6−8] but information on the temperature dependence of the branching fractions is lacking. In the present work we investigate the reactions of Cl with ethanol isotopomers,

$$Cl + CH_3CH_2OH \rightarrow HCl + CH_3CHOH \quad (1a)$$

$$\rightarrow HCl + CH_2CH_2OH \quad (1b)$$

$$\rightarrow HCl + CH_3CH_2O \quad (1c)$$

$$Cl + CD_3CH_2OH \rightarrow HCl + CD_3CHOH \quad (2a)$$

$$\rightarrow DCl + CD_2CH_2OH \quad (2b)$$

$$\rightarrow HCl + CD_3CH_2O \quad (2c)$$

$$Cl + CH_3CD_2OH \rightarrow DCl + CH_3CDOH \quad (3a)$$

$$\rightarrow HCl + CH_2CD_2OH \quad (3b)$$

$$\rightarrow HCl + CH_3CD_2O \quad (3c)$$

using the complementary techniques of laser photolysis/infrared long-path absorption and FTIR-smog chamber measurements. Absolute rate coefficients and HCl branching fractions for reactions 1−3 are reported between 295 and 600 K. The Cl + ethanol reaction has been exploited as a source for CH_3CHOH radicals.[5,7,9] The present measurements allow the branching fraction for α-abstraction (reaction 1a) and β-abstraction (reaction 1b) to be deduced between 295 and 600 K.

Time-Resolved Infrared Absorption Experiments at Sandia National Laboratories

The kinetics of the Cl + ethanol reactions (1−3) have been studied using the technique of laser photolysis/CW infrared

10.1021/jp992465l CCC: $18.00
Published on Web 11/12/1999

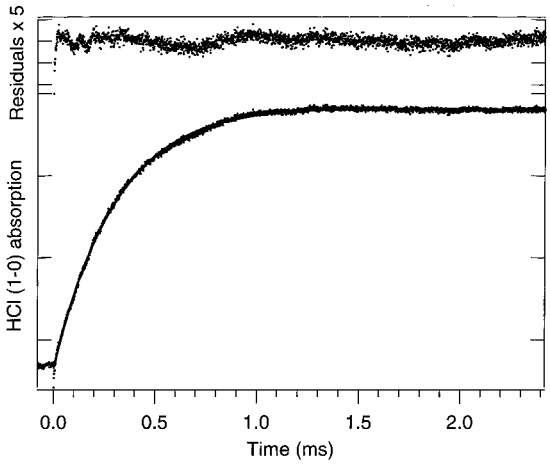

Figure 1. Time-resolved absorption on the P(2) line of the HCl (1 ← 0) transition following 193 nm photolysis of $CFCl_3/CH_3CD_2OH/CO_2$ mixture at 295 K. The peak absorption is ~0.2%; the concentration of CH_3CD_2OH is 4.35×10^{13} cm^{-3}. The solid line is a fit to a single-exponential form, with residuals (×5) displayed above.

absorption. The experimental method and apparatus are similar to previously reported experiments.[10−12] Briefly, the reaction is initiated by pulsed laser photolysis of CF_2Cl_2 or $CFCl_3$ at 193 nm. The formation of HCl product is monitored in time by a CW infrared probe beam tuned to the P(2) line of the $H^{35}Cl$ fundamental vibrational transition. The infrared beam is generated by difference-frequency mixing of two tunable diode lasers in periodically poled $LiNbO_3$.[13,14] The infrared laser is split into a signal and a reference beam, both of which are imaged onto matched InSb detectors. The signal beam is passed multiple times through the reaction cell using a Herriott-type multipass arrangement. The average power on the two detectors is made equal using an infrared polarizer to attenuate the reference beam. The time-resolved HCl production is then measured by the transient absorption (signal − reference) following the photolytic initiation. A typical time-resolved trace is shown in Figure 1. No time-resolved absorption signal is observed when the infrared carrier is tuned away from the HCl absorption by several gigahertz, indicating negligible contributions from absorption by other species. The contribution of scattered excimer laser light and radio-frequency (rf) pickup to the signal (visible as the prominent spike and subsequent ringing on the trace in Figure 1) is removed by subtraction of an off-resonance trace for more precise fitting of some traces with the highest time constants.

The reactor is a resistively heated stainless steel cell, equipped with multipass optics to increase the infrared absorption path. The multipass cell is based on the Herriott design[15,16] and allows long path lengths in conjunction with precise temperature control in the region of pump−probe overlap.[17] The CF_2Cl_2 or $CFCl_3$ photolyte, ethanol reactant, and buffer gas flows are controlled by separate calibrated mass flow controllers and enter the reactor through a common inlet at one end of the reactor. Calibration for CF_2Cl_2, $CFCl_3$, Ar, and CO_2 is carried out by calibrated volume displacement using a Hg-sealed piston in a NIST-traceable volumetric cylinder. Calibration of the ethanol flow is made by measuring the pressure rise in a glass bulb of known volume. The pressure in the reactor is controlled by a butterfly valve which operates under active feedback from a capacitance manometer. All of the experiments in this work are carried out at 10 Torr total pressure.

The CD_3CH_2OH and CH_3CD_2OH have a stated isotopic purity of 98%. The purity of all of the ethanol samples is tested by GC/MS and NMR analysis. Small (≤1%) impurities of normal ethanol and an unidentified organic contaminant occur in the deuterated ethanol samples. Corrections to the measured rate coefficients and HCl yields due to Cl reactions with these impurities are small and are discussed in the Results section. The ethanol is flowed as a pure vapor from above a liquid sample. Because of significant adsorption of ethanol on the walls of the stainless steel reactor, careful equilibration is necessary to ensure reproducible rate coefficient measurements. Only after a steady state is reached between adsorption and desorption on the walls is the composition governed by the relative flows into the reactor. Equilibration was ensured by repeatedly measuring the pseudo-first-order rate coefficient after each change of the ethanol flow and accepting results only after indistinguishable values are obtained for two successive averages (typically 200−500 shots each average). Equilibration times of up to 15 min were used in these experiments.

The initial Cl number density is approximately 10^{12} cm^{-3}, which is 30−300-fold lower than the ethanol reactant concentration, maintaining the pseudo-first-order limit. Typically, photolyte concentrations of $(5-25) \times 10^{14}$ cm^{-3} and photolysis fluences of ~1−5 mJ cm^{-2} are used. The peak absorption is kept below 5% (typically 0.5−1%) to ensure operation in the linear regime. Effects of secondary reactions of Cl atoms with reaction products are minimized by completely replenishing the reactant mixture between photolysis pulses. Spin−orbit excited $Cl[^2P_{1/2}]$ produced in the photolysis of CF_2Cl_2 or $CFCl_3$ is not expected to contribute significantly to the reaction kinetics, since the lifetime for $Cl[^2P_{1/2}]$ with respect to collisional quenching is approximately 6 μs at $[CF_2Cl_2] = 5 \times 10^{14}$ cm^{-3},[18] compared with typical reaction times of 80−1000 μs.

Absolute Rate Coefficient Measurements. For the general reaction of Cl with one of the ethanol isotopomers, the time profile of the HCl concentration is governed by the following kinetic equations:

$$\frac{d}{dt}[Cl] = -k[\text{ethanol}][Cl] - k_x[Cl] \quad (4)$$

$$\frac{d}{dt}[HCl] = \phi_{HCl}k[\text{ethanol}][Cl] - k_y[HCl] \quad (5)$$

where k_x represents all other removal processes for Cl including diffusion and reaction with buffer or photolyte impurities and k_y represents the removal of HCl, mainly by diffusion. The reaction rate coefficient k is the sum of all the product channels, and ϕ_{HCl} is the fraction of the reaction that produces HCl (e.g., $k = (k_{2a} + k_{2b} + k_{2c})$ and $\phi_{HCl} = (k_{2a} + k_{2c})/(k_{2a} + k_{2b} + k_{2c})$ for the Cl + CD_3CH_2OH reaction). These equations have the solution

$$[HCl]_t = \frac{[Cl]_0\phi_{HCl}k[\text{ethanol}]}{k[\text{ethanol}] + k_x - k_y}(e^{-k_y t} - e^{-(k[\text{ethanol}]+k_x)t}) \quad (6)$$

The time traces are therefore fit to the difference of two exponentials, where the rise time is related to the production rate of HCl, since in these experiments k[ethanol] > k_y. A plot of this time constant vs the ethanol concentration gives a straight line whose slope is k and whose intercept reflects losses of Cl atoms that do not depend on the ethanol concentration. Such a plot is shown in Figure 2 for the reaction of Cl + CH_3CH_2OH at room temperature.

Photolysis of ethanol at 193 nm is a possible source of error in the present measurements. The absorption of 193 nm light

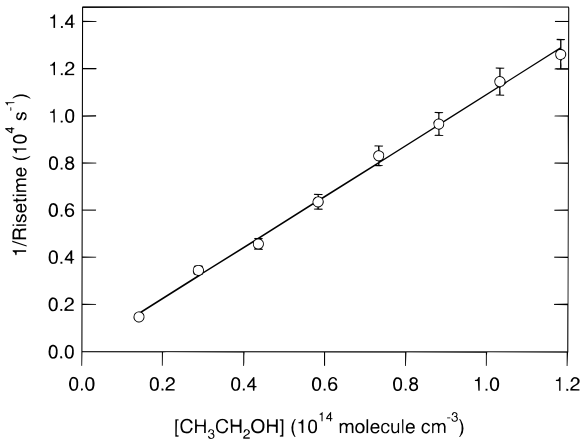

Figure 2. Plot of the inverse of the rise time of the HCl signal (i.e., the pseudo-first-order rate coefficient for HCl formation) vs ethanol concentration for the reaction of Cl with CH_3CH_2OH at 295 K. The slope of such a plot gives the second-order rate coefficient for the reaction.

by ethanol accesses a $\sigma^* \leftarrow$ n band and produces a hydrogen atom and an ethoxy radical.[19−21] The extent of ethanol photolysis is $\leq 10^{-3}$ so reactions of Cl with photoproducts is negligible compared to the Cl + ethanol reaction under study. Other reactions of the photolytically produced species affect the present measurements only insofar as they produce HCl. At higher excimer powers and higher ethanol concentrations, a much slower (time constants of 20−500 s^{-1}) additional component of HCl production is observed in some traces. This minor (<10%) slower component, presumably reflecting side chemistry (i.e., not involving Cl atoms) induced by ethanol photolysis, appears as a slightly sloping baseline and can be readily separated from the reactive signal. The reaction of H atoms with the counter-radical (CF_2Cl or $CFCl_2$) from the chlorofluoromethane photolysis is likely to be the largest source of spurious HCl signal in these experiments. Experiments with a maximum relative ethanol photolysis rate (i.e., $[\text{ethanol}]_{max}\sigma_{\text{ethanol},193}/[\text{photolyte}]\sigma_{\text{photolyte},193}$) from 0.02 to 0.45 give identical measured rate coefficients, confirming successful separation of any contributions of ethanol photolysis. However, ethanol photolysis is more prominent in the vibrational branching measurements, as discussed below.

Measurements of HCl Yield. Measurements of the HCl yield are performed by comparison with the Cl + propane or Cl + ethane reaction, where $\phi_{HCl} = 1$.[22] A measurement is made of the time profile of HCl formation from the reaction of Cl with the deuterated ethanol. The reactor is then pumped out to remove residual adsorbed ethanol. Subsequently, the experiment is repeated, with ethane or propane substituted for the deuterated ethanol, keeping the other conditions identical. Ethane and propane equilibrate much more rapidly than CH_3CH_2OH (which also has $\phi_{HCl} = 1$) and are hence more convenient references. Yield measurements are made at high values of the reactant concentration, so that $k[\text{ethanol}] \gg (k_x - k_y)$, and the amplitude in eq 6 reduces to $[Cl]_0\phi_{HCl}$. A comparison of the signal amplitudes for the ethane and the deuterated ethanol gives ϕ_{HCl} directly. Corrections due to absorption of the probe by ethane or by the deuterated ethanols are small compared to other errors.

The principal sources of random error in the yield measurement are changes in the total transmitted infrared intensity, frequency instability of the probe beam, and fluctuations in the photolysis power. Possible contributions from Cl reactions with background hydrogen-containing impurities and removal by diffusion can cause a systematic error in the yield, especially for low ϕ_{HCl}. The measured yields are corrected for this effect using the signal obtained at "zero reagent", that is, with only photolyte and buffer flows after the reactor has been pumped out to reduce adsorbed ethanol. This correction is less than 0.5% and is much smaller than the random errors. Measurements of the HCl yield for CD_3CH_2OH and CH_3CD_2OH are carried out at concentrations where the rise time is $\geq 10\,000$ s^{-1}, approximately 100 times the zero reagent rise time (typically ~100 s^{-1}). Upper limits on the HCl yield for CD_3CD_2OH are measured at similar concentrations, but the signal-to-noise is insufficient to determine a precise rise time for HCl production.

Vibrationally Excited HCl. The infrared absorption probe is inherently sensitive to vibrational excitation in the HCl product, and this sensitivity has been exploited in previous experiments to determine vibrational branching fractions.[23,24] The reaction of Cl atoms with ethanol is only mildly exothermic,[25] and the production of HCl ($v = 1$) is expected to be small. Nonetheless, production of vibrationally excited HCl is observed. The infrared absorption signal is proportional to the degeneracy-weighted difference in population between the two levels linked by the transition, e.g., for the P(2) line used in the present study, between ($v = 0$, $J = 2$) and ($v = 1$, $J = 1$). As a consequence, any deviation from a thermal vibrational population will change the proportionality between the probe signal and the total HCl population. The time-resolved signal will then reflect a convolution of vibrational energy transfer and changes in the HCl concentration. Measurements of the rate coefficient are taken in 10 Torr of CO_2 buffer, which rapidly relaxes HCl ($v = 1$) ($k \sim 3 \times 10^{-13}$ cm^3 $molecule^{-1}$ s^{-1}) and maintains vibrational thermal equilibrium.[26] Experiments in Ar buffer, where vibrational relaxation is relatively slow ($k \leq 10^{-17}$ cm^3 $molecule^{-1}$ s^{-1}), allow the production of vibrationally excited HCl to be investigated.

When Ar is used as the buffer gas, the relaxation of vibrationally excited HCl is dominated by collisions with the ethanol reagent (with some rate coefficient k_{VET}), since vibrational energy transfer from HCl ($v = 1$) is inefficient with the photolyte as well as with Ar. Rotational relaxation, on the other hand, is essentially instantaneous, and the rotations remain in thermal equilibrium. For a reaction producing a fraction f of vibrationally excited HCl, $f \equiv \text{HCl}(v{=}1)/\text{HCl(total)}$, the time profiles of HCl ($v = 0$) and ($v = 1$) are then given by the following equations:

$$\frac{[\text{HCl}(v=1)]_t}{[\text{Cl}]_0\phi_{\text{HCl}}} = \frac{fk(e^{-k_{\text{VET}}[\text{ethanol}]t} - e^{-k[\text{ethanol}]t})}{k - k_{\text{VET}}} \quad (7a)$$

$$\frac{[\text{HCl}(v=0)]_t}{[\text{Cl}]_0\phi_{\text{HCl}}} = 1 + \frac{(k_{\text{VET}} - (1-f)k)e^{-k[\text{ethanol}]t}}{k - k_{\text{VET}}} - \frac{fke^{-k_{\text{VET}}[\text{ethanol}]t}}{k - k_{\text{VET}}} \quad (7b)$$

The absorption on the P(2) line of the $v = 1 \leftarrow 0$ transition is proportional to the degeneracy-weighted difference between the populations in the upper ($v = 1$, $J = 1$) and lower ($v = 0$, $J = 2$) levels.

$$\text{absorption}_{(1\leftarrow 0)} \propto 1 - \frac{(1+\epsilon)fk}{k - k_{\text{VET}}}e^{-k_{\text{VET}}[\text{ethanol}]t} + \left[\frac{(1+\epsilon)fk}{k - k_{\text{VET}}} - 1\right]e^{-k[\text{ethanol}]t} \quad (8)$$

where ϵ is a correction for the different rotational Boltzmann fractions in the upper and lower levels,

$$\epsilon = \frac{Q_{\mathrm{rot}}^{\upsilon=1} e^{-J_{\mathrm{lower}}(J_{\mathrm{lower}}+1)B_{v=0}/k_B T}}{Q_{\mathrm{rot}}^{\upsilon=0} e^{-J_{\mathrm{upper}}(J_{\mathrm{upper}}+1)B_{v=1}/k_B T}} \quad (9)$$

Here Q is a rotational partition function, k_B is the Boltzmann constant, and B is a rotational constant. Once the total rate coefficient has been independently measured from experiments in CO_2, the absorption on the (1 ← 0) line can in principle be used to determine both f and k_{VET}.[23] Production of HCl(υ=2) is energetically excluded in the Cl + ethanol reaction, so the (2 ← 1) absorption should be proportional to the HCl(υ=1) concentration in eq 7a. Therefore, in the absence of some competing reaction that produces HCl(υ>1), the rise (or fall if $k_{VET} > k$) of the (2 ← 1) absorption should reflect the total rate coefficient k, measured in CO_2. In the present experiments, where HCl(υ=1) is a minor component, the time profile of the (2 ← 1) absorption is particularly important in discriminating against contributions from side reactions.

FTIR Smog Chamber System at Ford Motor Company

All experiments were performed in a 140 L Pyrex reactor interfaced to a Mattson Sirus 100 FTIR spectrometer.[27] The optical path length of the infrared beam was 27 m. The reactor was surrounded by 22 fluorescent blacklamps (GE F15T8-BL) which were used to photochemically initiate the experiments. Cl atoms were generated by the photolysis of molecular chlorine in 700 Torr total pressure of N_2 diluent at 296 ± 2 K.

$$Cl_2 \rightarrow 2Cl \quad (10)$$

$$Cl + C_2H_5OH \rightarrow \text{products} \quad (1)$$

Loss of C_2H_5OH and formation of products were measured by FTIR spectroscopy at a resolution of 0.25 cm^{-1}. Typically, IR spectra were derived from 32 co-added interferograms. For experiments performed to investigate the decomposition of $CH_3CHClOH$, the IR spectra were recorded at resolutions of 0.5−2 cm^{-1} using 4−10 co-added interferograms (the acquisition time was 8−20 s). Reference spectra of CH_3CHO, $CH_3C(O)Cl$, and CH_2ClCH_2OH were generated by expanding known volumes of these compounds into the chamber. Spectral subtractions of CH_3CHO, $CH_3C(O)Cl$, and CH_2ClCH_2OH were performed using their characteristic features at 1746, 1820, and 1201 cm^{-1}, respectively.

Results

Time-Resolved Infrared Measurements of Absolute Rate Coefficients and HCl Yields. The measured rate coefficients for Cl reacting with ethanol isotopomers are summarized in Table 1 and Figure 3. The statistical error of the individual determinations (±2σ) is ≤5%, using 8−10 concentrations of ethanol as shown in Figure 2. This uncertainty is convoluted with estimates of possible errors in total pressure, temperature, and concentration measurements, as well as uncertainties associated with possible systematic errors discussed in the previous section, to arrive at the reported ±2σ error limits. The rate coefficients for all three reactions measured show only a slight temperature dependence, with the Cl + CH_3CH_2OH and Cl + CD_3CH_2OH reactions showing more negative activation energies than the Cl + CH_3CD_2OH reaction. The rate coefficients can be parametrized by the Arrhenius functions $k_1 = (9.4 \pm 1.4) \times 10^{-11} e^{(45 \pm 32)/T}$ cm^3 $molecule^{-1}$ s^{-1}, $k_2 = (6.6 \pm 0.9) \times 10^{-11} e^{(90 \pm 40)/T}$ cm^3 $molecule^{-1}$ s^{-1}, and $k_3 = (6.9 \pm 0.7) \times 10^{-11} e^{(-76 \pm 40)/T}$ cm^3 $molecule^{-1}$ s^{-1} over the temperature range studied, where the error estimates refer to the precision of the fit to Arrhenius form, weighted by the propagated uncertainties in the individual determinations. Corrections to the rate coefficients for measured impurities in the ethanol samples are negligible for CH_3CH_2OH and CD_3CH_2OH; the major impurity in the deuterated ethanol is normal ethanol (≤1%), which reacts at a similar rate to CD_3CH_2OH. The rate coefficient for CH_3CD_2OH may be influenced to a greater degree, since its rate coefficient is smaller, but the correction is still at the 1−2% level and can be neglected relative to the random uncertainties in the measurement.

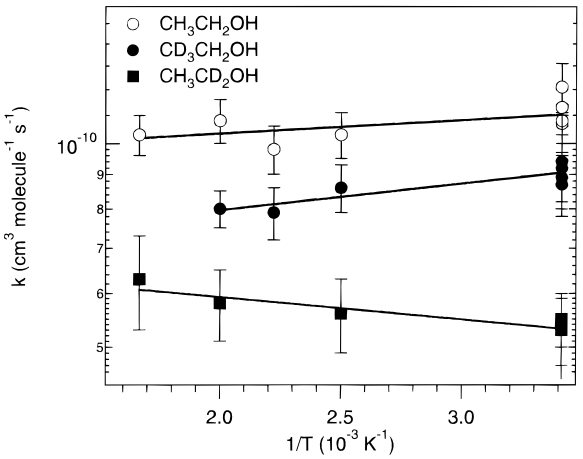

Figure 3. Rate coefficients for the reactions of Cl atoms with ethanol isotopomers. The error bars represent the precision of the individual determinations.

TABLE 1: Rate Coefficients for the Reactions of Cl with Ethanol Isotopomers[a]

temp (K)	k_1[b]	k_2[b]	k_3[b]
295	10.9 ± 0.9	9.0 ± 0.9	5.4 ± 0.5
400	10.3 ± 0.9	8.6 ± 0.9	5.6 ± 0.7
450	9.8 ± 0.8	7.9 ± 0.8	
500	10.8 ± 0.9	8.0 ± 0.8	5.8 ± 0.7
600	10.3 ± 0.9		6.3 ± 0.8

[a] Error bars are ±2σ and include estimates of systematic error. [b] Units of 10^{-11} cm^3 $molecule^{-1}$ s^{-1}.

TABLE 2: Measured HCl Yields, ϕ_{HCl}, for Cl Reactions with Selectively Deuterated Ethanols[a]

temp (K)	CD_3CH_2OH	CH_3CD_2OH	CD_3CD_2OH
295	0.95 ± 0.1	0.16 ± 0.04	<0.05
400	1.03 ± 0.1	0.18 ± 0.05	<0.05
450	0.92 ± 0.1	0.20 ± 0.05	
500	0.99 ± 0.1	0.26 ± 0.08	
550	0.95 ± 0.1		
600		0.22 ± 0.05	

[a] Error bars are ±2σ and include estimates of systematic error.

The yields of HCl in the reactions of Cl atoms with partially deuterated ethanols are listed in Table 2. The observed yield in the reaction of Cl with CH_3CD_2OH has been corrected for the presence of 1% CH_3CH_2OH. Since CH_3CH_2OH reacts twice as fast as CH_3CD_2OH with Cl atoms, a contamination of 1% normal ethanol will contribute approximately 2% to the observed HCl yield. The observed yields are corrected to the actual yield for Cl + CH_3CD_2OH using $\phi_{HCl}(\text{observed}) \approx 0.98\phi_3 + 0.02$, where the notation ϕ_3 refers to the HCl yield for reaction 3, i.e., $\phi_3 \equiv \phi_{HCl}(CH_3CD_2OH)$. The yield of HCl in the reaction of Cl with CD_3CH_2OH is nearly unity, so the similar correction, $\phi_{HCl}(\text{observed}) \approx 0.99\ \phi_2 + 0.01$, has an essentially negligible effect. Measurements of the HCl yield for Cl + CD_3CD_2OH

were also carried out; the HCl produced in this reaction is exceedingly small, and the reported measurement is an upper limit.

Combining the HCl yields and the measured rate coefficients allows the kinetic isotope effects and site-specific rate coefficients to be deduced. In the absence of secondary isotope effects, the product of the HCl yields and rate coefficients for a partially deuterated ethanol gives the rate coefficient for the nondeuterated sites. For example, $\phi_3 k_3 = k_{CH_3} + k_{OH}$. However, abstraction at the OH is slightly endothermic and is expected to be disfavored relative to the exothermic pathways available in the Cl + ethanol reaction. The signal-to-noise for the Cl + CD_3CD_2OH reaction is too poor to allow a rate coefficient to be measured, but if we assume similar kinetic isotope effects to the other ethanol isotopomers, $k_{CD_3CD_2OH}$ should be approximately $0.45k_1$. Using the current measurements of $\phi_{HCl}(CD_3CD_2OH) \leq 0.05$ places an upper limit of 2% for reaction at the OH site. The contribution from O−H abstraction can therefore be neglected. The relative contribution of the $-CH_3$ group in the Cl + ethanol reaction is then given by $k_{CH_3}/k_1 \sim \phi_3 k_3/k_1 = 0.08 \pm 0.02$ (2σ), which is in excellent agreement with the FTIR product measurements, as described below.

The magnitude of any secondary kinetic isotope effect in the reaction can be judged by comparing the sums of the apparent site-specific rate coefficients with the measured Cl + CH_3CH_2OH rate coefficient. If secondary kinetic isotope effects can be neglected (and ignoring reaction of the OH group),

$$\phi_3 k_3 + \phi_2 k_2 = k_1 \tag{11}$$

Using the values of the yields and rate coefficients from Tables 1 and 2, the sum of the apparent site-specific rate coefficients (left-hand side of eq 11) is slightly smaller than the measured k_1 but lies within the propagated uncertainties. Small secondary kinetic isotope effects have been measured for the similar system of Cl reacting with partially deuterated ethyl chloride,[28] but in reactions of OH with selectively deuterated propanes, no secondary isotope effect was observed.[29]

Again treating the secondary isotope effect as negligible, the kinetic isotope effect for the individual sites can be derived:

$$\frac{k_{CH_2}}{k_{CD_2}} = \frac{\phi_2 k_2}{(1-\phi_3)k_3} \tag{12}$$

The isotope effect at the CH_2 site is 1.9 ± 0.3 (2σ) at 295 K and is constant to within the experimental uncertainty over the temperature range of the current experiments. The yield measurement ϕ_2 is not precise enough for $(1 - \phi_2)$ to be meaningful; hence, the kinetic isotope effect for the methyl group cannot be determined in an analogous fashion.

Vibrationally Excited HCl. Production of vibrationally excited HCl has been measured in reactions 1 and 2. Nonequilibrium vibrational populations in the HCl product can be inferred from a buffer dependence of the apparent reaction rate coefficient or a nonexponential rise in the HCl absorption signal. The production of excited HCl can be directly confirmed by tuning the infrared probe laser to a transition arising from $v = 1$. Figure 4 shows a time-resolved absorption trace taken on the P(2) line of the HCl ($1 \leftarrow 0$) transition for Cl reacting with CD_3CH_2OH in Ar buffer. Under these conditions, the vibrational relaxation of HCl is relatively slow. The top trace, Figure 4a, shows a simple exponential fit to the time profile. As can be seen in the residuals, there is a systematic deviation from single-exponential behavior in the HCl production. The lower trace,

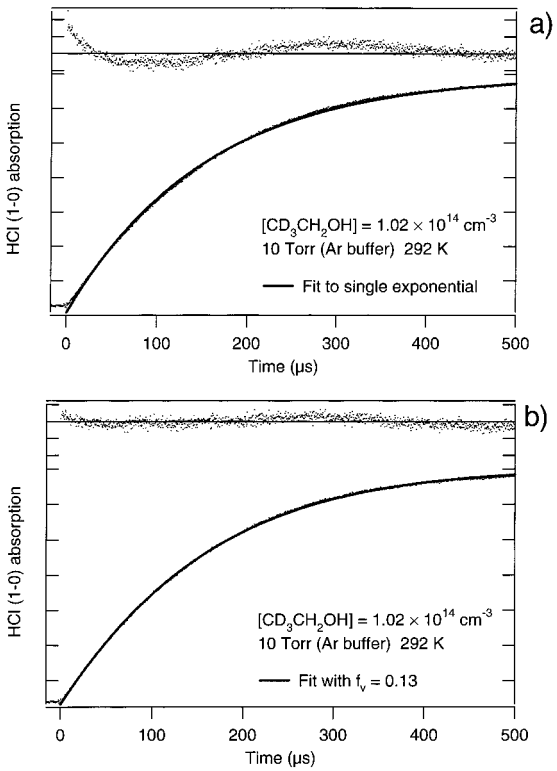

Figure 4. Time-resolved absorption on the P(2) line of the HCl ($1 \leftarrow 0$) transition following 193 nm photolysis of CF_2Cl_2/CD_3CH_2OH/Ar mixture at 295 K. (a**)** Fit to a simple exponential form, which ignores possible contributions of HCl ($v = 1$). Residuals ($\times 5$) are displayed above. There is a systematic deviation of the signal from single-exponential behavior which is particularly visible in the residuals at early times. (b**)** Fit taking HCl ($v = 1$) into account. Residuals ($\times 5$) are displayed above. The fit is considerably improved. Such a fit is used to extract HCl ($v = 1$) branching fractions (see text for details).

Figure 4b, shows a fit to eq 8, using the rate coefficient k_2 measured in CO_2 buffer. The vibrational branching fraction f = HCl(v=1)/HCl(total) extracted from this fit is 0.13. The accuracy of the vibrational fraction determined using eq 8 depends on the accuracy of the total rate coefficient, which is determined in CO_2. A change of 20% in the total rate coefficient changes the vibrational branching by a few percent. The fraction of HCl product observed in $v = 1$ is 0.14 ± 0.04 for Cl + CD_3CH_2OH and 0.19 ± 0.05 for Cl + CH_3CH_2OH, where the $\pm 2\sigma$ error estimates are based on the precision of the individual determinations and the uncertainties in the total rate coefficients.

Figure 5 shows the time-resolved absorption on the R(2) line of the HCl ($2 \leftarrow 1$) transition, taken for Cl reacting with CH_3CH_2OH in Ar buffer, confirming the production of HCl(v=1) in the reaction. Similar traces are observed for Cl + CD_3CH_2OH. The relative magnitudes of the ($2 \leftarrow 1$) and ($1 \leftarrow 0$) absorptions are consistent with the vibrational branching fractions determined from the time behavior of the ($1 \leftarrow 0$) signal. In Ar buffer, the vibrational relaxation is governed principally by collisions of HCl(v=1) with the ethanol reagent. The solid line in Figure 5 is a fit to the difference of two exponentials (eq 7a), fixing the total rate coefficient k to the value measured in CO_2. The vibrational relaxation rate coefficient, k_{VET}, can also be deduced from such a fit. The time constants that are extracted from these fits are relatively imprecise because of the low signal-to-noise and the near-degeneracy of the two time constants (eq 7a diverges when $k = k_{VET}$). The value for k_{VET} obtained from a plot of the pseudo-first-order vibrational

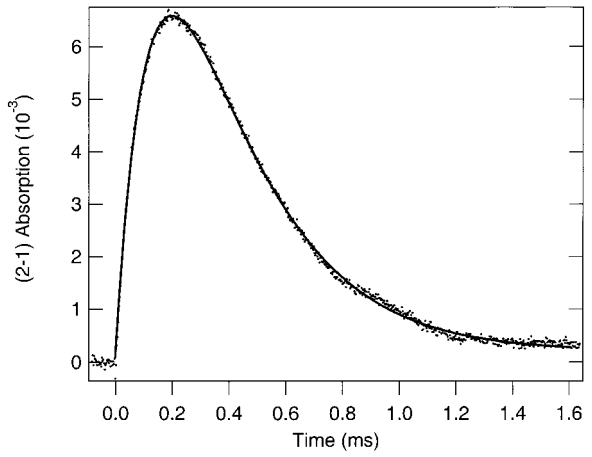

Figure 5. Time-resolved absorption from HCl ($v = 1$), using the R(2) line of the HCl ($2 \leftarrow 1$) transition, following 193 nm photolysis of $CFCl_3/CD_3CH_2OH/Ar$ mixture at 295 K. The solid line is a fit using the total rate coefficient for HCl formation as measured in CO_2 buffer, where HCl ($v = 1$) is rapidly relaxed.

relaxation rate coefficients vs ethanol concentration is $(8 \pm 4) \times 10^{-11}$ cm^3 molecule^{-1} s^{-1} (2σ) for both CD_3CH_2OH and CH_3CH_2OH.

A search was made for vibrationally excited HCl from the reaction of Cl with CH_3CD_2OH, but only a small HCl ($v = 1$) signal from a secondary reaction could be observed. The secondary reaction is distinguished by a sigmoidal rise of the ($2 \leftarrow 1$) absorption signal which does not match the total reaction rate measured in CO_2 buffer. Some secondary reaction contribution could be seen in the Cl + CD_3CH_2OH HCl ($v = 1$) signal at high ethanol concentrations and 193 nm photon fluxes but could be made negligible at lower excimer power. Some ethanol photolysis, producing ethoxy + H, is unavoidable in the present experiments; hence, one possible source of the HCl ($v = 1$) contaminant is radical−radical reactions of H + CF_2Cl and $CFCl_2$. The H + CF_2Cl reaction is known to produce high levels of vibrational excitation in the HCl product,[30] and vibrational cascade would produce a sigmoidal appearance to the absorption. The HCl yield is much smaller for reaction 3 than for reaction 2, making any contribution from competing reactions more prominent; in addition, abstraction from the CH_3 group is less exothermic than abstraction from the $-CH_2-$ group, and the HCl ($v = 1$) contribution should be much smaller. The magnitude of the secondary HCl ($2 \leftarrow 1$) absorption corresponds to HCl concentrations of less than 1% of the initial Cl atom concentration. From the lack of direct ($2 \leftarrow 1$) absorption in reaction 3, an upper limit of $f < 0.03$ can be placed on the HCl ($v = 1$) fraction from Cl + CH_3CD_2OH.

Smog Chamber Relative Rate Measurements of k_2. The kinetics of reaction 2 were measured relative to reactions 13 and 1.

$$\mathrm{Cl} + \mathrm{CD_3CH_2OH} \rightarrow \text{products} \qquad (2)$$

$$\mathrm{Cl} + \mathrm{C_2H_6} \rightarrow \text{products} \qquad (13)$$

$$\mathrm{Cl} + \mathrm{C_2H_5OH} \rightarrow \text{products} \qquad (1)$$

Initial concentrations were 51−107 mTorr of CD_3CH_2OH, 74−518 mTorr of Cl_2, 52−108 mTorr of C_2H_6, and 46−64 mTorr of C_2H_5OH, in 700 Torr of either O_2 or N_2 diluent. The observed loss of CD_3CH_2OH versus the reference compounds in the presence of Cl atoms is shown in Figure 6. Linear least-squares analysis of the data in Figure 6 gives $k_2/k_{13} = 1.60 \pm 0.08$ and

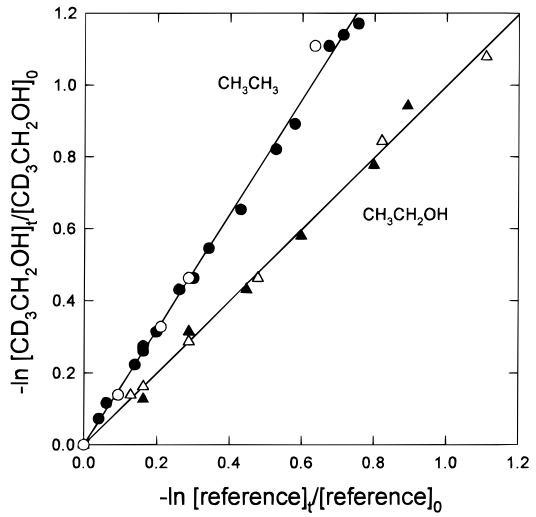

Figure 6. Loss of CD_3CH_2OH versus loss of CH_3CH_3 (circles) and CH_3CH_2OH (triangles) in the presence of Cl atoms. Experiments were performed at 296 K in 700 Torr of N_2 (filled symbols), O_2 diluent (open circles), or air diluent (open circles).

$k_2/k_1 = 1.00 \pm 0.06$ (2σ). Using the recommended values for $k_{13} = 5.9 \times 10^{-11}$ and $k_1 = 9.0 \times 10^{-11}$,[31] we derive $k_2 = (9.4 \pm 0.5) \times 10^{-11}$ and $k_2 = (9.0 \pm 0.5) \times 10^{-11}$ cm^3 molecule^{-1} s^{-1}. We estimate that potential systematic errors associated with uncertainties in the reference rate constants add 10% to the uncertainty range for k_2. Propagating this additional uncertainty gives $k_2 = (9.4 \pm 1.1) \times 10^{-11}$ cm^3 molecule^{-1} s^{-1}, using the better characterized k_{13} as the preferred reference reaction. The quoted $\pm 2\sigma$ error reflects the accuracy of the measurements. Use of the present absolute result for k_1 in conjunction with the measured k_2/k_1 ratio would yield a slightly larger value, $k_2 = (10.9 \pm 1.2) \times 10^{-11}$ cm^3 molecule^{-1} s^{-1}.

FTIR Product Study of the Reaction of Cl Atoms with C_2H_5OH. To investigate the mechanism of reaction 1, experiments were performed using UV irradiation of $CH_3CH_2OH/Cl_2/N_2$ mixtures. Initial concentrations were 13−127 mTorr of Cl_2 and 45−135 mTorr of C_2H_5OH in 700 Torr of N_2. In such experiments CH_2ClCH_2OH and $CH_3CHClOH$ are produced by photolysis of $C_2H_5OH/Cl_2/N_2$ mixtures by the following sequence of reactions[32,33]

$$\mathrm{Cl_2} + h\nu \rightarrow 2\mathrm{Cl} \qquad (14)$$

$$\mathrm{Cl} + \mathrm{CH_3CH_2OH} \rightarrow \mathrm{CH_3CH(\bullet)OH} + \mathrm{HCl} \qquad (1a)$$

$$\mathrm{Cl} + \mathrm{CH_3CH_2OH} \rightarrow \bullet\mathrm{CH_2CH_2OH} + \mathrm{HCl} \qquad (1b)$$

$$\bullet\mathrm{CH_2CH_2OH} + \mathrm{Cl_2} \rightarrow \mathrm{CH_2ClCH_2OH} + \mathrm{Cl} \qquad (15)$$

$$\mathrm{CH_3CH(\bullet)OH} + \mathrm{Cl_2} \rightarrow \mathrm{CH_3CHClOH} + \mathrm{Cl} \qquad (16)$$

The yields of CH_2ClCH_2OH and $CH_3CHClOH$ provide a measure of the importance of channels 1b and 1a. By analogy to the reaction of Cl atoms with methanol, which proceeds exclusively via attack on the CH_3 group,[1,2]

$$\mathrm{Cl} + \mathrm{CH_3OH} \rightarrow \bullet\mathrm{CH_2OH} + \mathrm{HCl} \qquad (17)$$

hydrogen abstraction from the −OH group is not expected to be of any significance in the reaction of Cl atoms with ethanol. Direct observation of the HCl yield in the reaction of Cl with CD_3CD_2OH (above) confirms that reaction at the OH site is negligible. In smog chamber experiments unwanted loss of

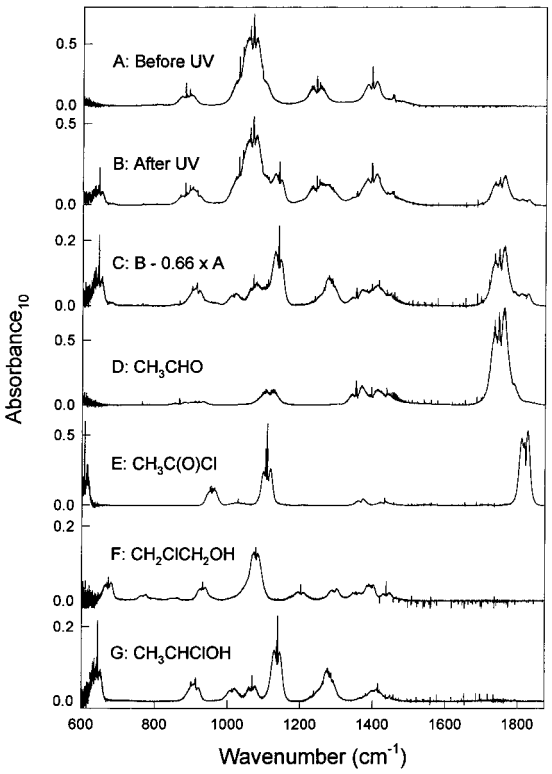

Figure 7. Infrared spectra acquired before (A) and after (B) a 3 s irradiation of a mixture of 59.8 mTorr of CH_3CH_2OH and 80 mTorr of Cl_2 in 700 Torr of N_2 diluent. Subtraction of features attributable to CH_3CH_2OH gives panel C. Panels D, E, and F show reference spectra of CH_3CHO, $CH_3C(O)Cl$, and CH_2ClCH_2OH, respectively. Subtraction of IR features of CH_3CHO, $CH_3C(O)Cl$, and CH_2ClCH_2OH from panel C gives the product spectrum in panel G, which is assigned to $CH_3CHClOH$ (at a partial pressure of 7.3 mTorr).

reactants and products via photolysis, dark chemistry, and heterogeneous loss by surface reactions have to be considered. Control experiments were performed to check for such losses of C_2H_5OH and CH_2ClCH_2OH. No loss was observed when these compounds were subjected to UV irradiation in N_2 diluent or when mixtures containing these compounds and Cl_2 were left to stand in the dark. However, it was observed that $CH_3CHClOH$ decomposes rapidly (~1 min) when left in the dark in the chamber.

Following photolysis of $C_2H_5OH/Cl_2/N_2$ mixtures, three products (CH_3CHO, $CH_3C(O)Cl$, and CH_2ClCH_2OH) were readily identified and quantified using calibrated reference spectra. Figure 7 shows spectra acquired before (A) and after (B) a 3 s irradiation of a mixture of 59.8 mTorr of C_2H_5OH and 80 mTorr of Cl_2 in 700 Torr of N_2 diluent. Subtraction of IR features attributable to C_2H_5OH, CH_3CHO, $CH_3C(O)Cl$, and CH_2ClCH_2OH from panel B gives the product spectrum in panel G. All features in panel G appear and disappear at the same rate, suggesting that this is a spectrum of only one compound. We therefore assign the spectrum in panel G to $CH_3CHClOH$. When reaction mixtures were left in the dark, $CH_3CHClOH$ disappeared rapidly (with a lifetime of ~1 min), resulting in formation of CH_3CHO and HCl. The concentrations of C_2H_5OH, CH_2ClCH_2OH, and $CH_3C(O)Cl$ remained constant in the dark. This observation suggests that $CH_3CHClOH$ decomposes via HCl elimination in a manner similar to the decomposition of chlorinated methanols, CH_2ClOH to give HCHO and HCl, $CHCl_2OH$ to give HC(O)Cl and HCl, and CCl_3OH to give $COCl_2$ and HCl:[32,33]

$$CH_3CHClOH \xrightarrow{\Delta} CH_3CHO + HCl \qquad (18)$$

Figure 8 shows that the loss of $CH_3CHClOH$ scales linearly with the formation of CH_3CHO in the dark. This linear relationship was used to calibrate the $CH_3CHClOH$ yield. (The spectrum shown in Figure 7G corresponds to a partial pressure of 7.3 mTorr.) At 912.3 cm^{-1} we report $\sigma(CH_3CHClOH) = 2.2 \times 10^{-19}$ cm^2 $molecule^{-1}$. In principle, it is possible that reaction 18 occurs as a homogeneous gas-phase reaction (the change in Gibbs free energy is $\Delta G_{298} = -9.1$ kcal mol^{-1}).[34] Experiments were performed to follow the decomposition of $CH_3CHClOH$ using short data acquisition times. As shown in the inset to Figure 8, for a given experiment the loss of $CH_3CHClOH$ followed first-order kinetics. However, the decay rate constant obtained in different experiments varied over the range $(1.5-4.0) \times 10^{-2}$ s^{-1} and was not reproducible. Such behavior is consistent with the reaction proceeding largely, if not entirely, via a heterogeneous mechanism similar to that reported for CH_2ClOH, $CHCl_2OH$, and CCl_3OH with the rate sensitive to the condition of the reactor walls.[33]

Acetaldehyde is almost as reactive toward Cl atoms as ethanol (recommended rate coefficients are $k_{19} = 7.2 \times 10^{-11}$ cm^3 $molecule^{-1}$ s^{-1} and $k_1 = 9.0 \times 10^{-11}$ cm^3 $molecule^{-1}$ s^{-1}).[31] During the UV irradiation of $Cl_2/C_2H_5OH/N_2$ mixtures it is expected that acetaldehyde will be converted into acetyl chloride via reactions 19 and 20,

$$CH_3CHO + Cl \rightarrow CH_3C(O)\bullet + HCl \qquad (19)$$

$$CH_3C(O)\bullet + Cl_2 \rightarrow CH_3C(O)Cl + Cl \qquad (20)$$

and that the $[CH_3C(O)Cl]/[CH_3CHO]$ ratio will increase with conversion of ethanol. This is indeed the behavior that was observed. The $[CH_3C(O)Cl]/[CH_3CHO]$ ratio increased with the conversion of ethanol whereas the sum of the CH_3CHO, $CH_3C(O)Cl$, and $CH_3CHClOH$ concentrations scaled linearly with the loss of ethanol, as can be seen in the inset to Figure 9.

For the ethanol consumption used here (10−70%) secondary loss of CH_2ClCH_2OH via reaction 21 is of minor importance ($k_{21} = 3 \times 10^{-11}$ cm^3 $molecule^{-1}$ s^{-1}).[35]

$$Cl + CH_2ClCH_2OH \rightarrow \text{products} \qquad (21)$$

The formation of CH_2ClCH_2OH scales linearly with the loss of CH_3CH_2OH as shown in Figure 9. A linear least-squares fit to the data gives a CH_2ClCH_2OH yield of 0.072 ± 0.002 ($\pm 2\sigma$). Since the CH_2ClCH_2OH yield was quantified from very weak absorption bands, the uncertainty due to systematic subtraction errors is estimated at 20%. The uncertainty in the calibration of the CH_2ClCH_2OH reference spectrum is estimated to be 5%. Propagating these additional uncertainties gives a CH_2ClCH_2OH yield of 0.072 ± 0.015. The inset of Figure 9 shows the sum of the CH_3CHO, $CH_3C(O)Cl$, CH_2ClCH_2OH, and $CH_3CHClOH$ concentrations versus ethanol loss; the total carbon balance is 95 ± 5%. We conclude that $k_{1b}/k_1 = 0.07 \pm 0.02$ ($\pm 2\sigma$) with the balance of the occurring via channel k_{1a}.

Discussion

The present work provides the first absolute rate data for reaction of Cl atoms with ethanol and is the first kinetic study of this reaction at temperatures other than ambient. Using relative rate techniques, Wallington et al.[4] and Edelbuttel-Einhaus et al.[5] reported $k_1/k_{13} = 1.48 \pm 0.16$ and 1.4 ± 0.3 which, combined with $k_{13} = 5.9 \times 10^{-11}$ cm^3 $molecule^{-1}$ s^{-1},[31]

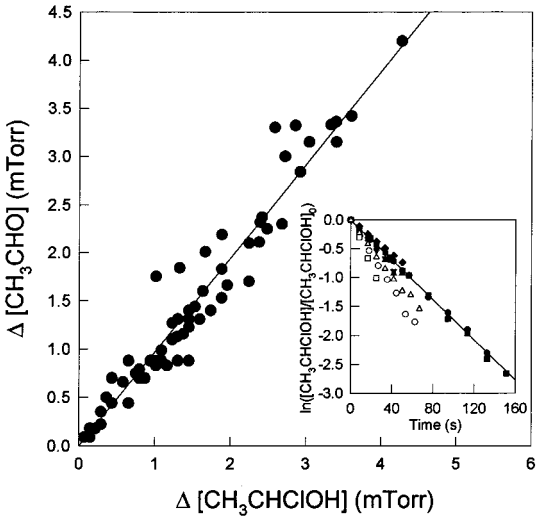

Figure 8. Formation of CH_3CHO versus loss of $CH_3CHClOH$ when reaction mixtures were allowed to stand in the dark (see text for details). Inset: decay of $CH_3CHClOH$ as a function of time in the dark.

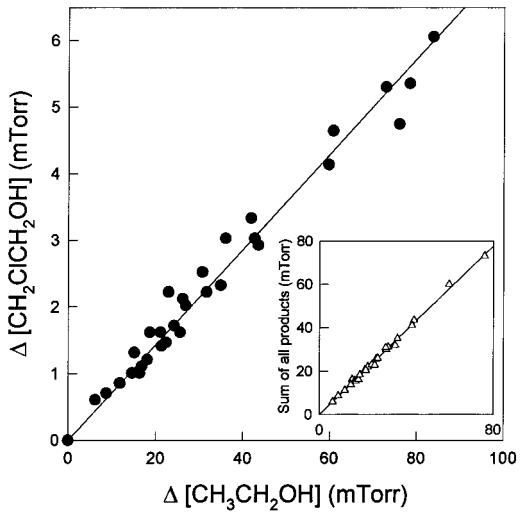

Figure 9. Formation of CH_2ClCH_2OH versus loss of CH_3CH_2OH from UV irradiation of mixtures of 13−127 mTorr of Cl_2 and 45−135 mTorr of CH_3CH_2OH in 700 Torr of N_2 diluent. Inset: the sum of products CH_3CHO, $CH_3C(O)Cl$, $CH_3CHClOH$, and CH_2ClCH_2OH versus loss of CH_3CH_2OH from UV irradiation of mixtures of 13−127 mTorr of Cl_2 and 45−135 mTorr of CH_3CH_2OH in 700 Torr of N_2 diluent.

give $k_1 = (8.7 \pm 0.9)$ and $(8.3 \pm 1.8) \times 10^{-11}$ cm^3 molecule^{-1} s^{-1}, respectively. In another relative rate study, Nelson et al. used the reaction of Cl with cyclohexane as reference,

$$\mathrm{Cl} + \text{c-}\mathrm{C_6H_{12}} \rightarrow \text{products} \qquad (22)$$

and reported $k_1 = (10.1 \pm 0.6) \times 10^{-11}$ cm^3 molecule^{-1} s^{-1}, using $k_{22} = 3.11 \times 10^{-10}$ cm^3 molecule^{-1} s^{-1}.[3] Combining the present relative rate measurements of $k_2/k_1 = 1.00 \pm 0.06$ and $k_2/k_{13} = 1.60 \pm 0.08$ gives $k_1/k_{13} = 1.60 \pm 0.13$ and hence $k_1 = (9.4 \pm 0.8) \times 10^{-11}$ cm^3 molecule^{-1} s^{-1}. For reasons that are unclear, the present absolute measurement of $k_1 = (10.9 \pm 0.9) \times 10^{-11}$ cm^3 molecule^{-1} s^{-1} falls slightly (about 15%) higher than the results from the relative rate studies. There being no obvious reason to prefer any one study over the others, we recommend a value of $k_1(298\ \mathrm{K}) = 9.5 \times 10^{-11}$ cm^3 molecule^{-1} s^{-1} with an estimated uncertainty of ±20%. Further absolute measurements of this rate constant by independent methods are warranted.

The temperature dependence of reactions 1−3 is shallow, as observed in similarly exothermic Cl + hydrocarbon abstractions.[12,31] The smog chamber measurement of Cl + CD_3CH_2OH relative to ethane reported here gives a rate coefficient at 295 K of $k_2 = (9.4 \pm 1.1) \times 10^{-11}$ cm^3 molecule^{-1} s^{-1}, in excellent agreement with the present absolute rate coefficient measurement of $k_2 = (9.0 \pm 0.9) \times 10^{-11}$ cm^3 molecule^{-1} s^{-1}.

The effect of deuteration at the CH_2 site, $k_{CH_2}/k_{CD_2} = 1.9 \pm 0.3$ (2σ), is similar to that observed for the analogous α-hydrogen abstraction in chloroethane, where $k_{CH_2}/k_{CD_2} = 2.30 \pm 0.10$ at 280 K and 2.16 ± 0.09 (2σ) at 325 K.[36] However, since β-abstraction is a minor channel, the deuterium kinetic isotope effect for abstraction at the methyl group is not well-determined by the present experiments. The smog chamber measurements of the relative rates of Cl + CD_3CH_2OH (k_2) and Cl + CH_3CH_2OH (k_1) appear to preclude more than a very small kinetic isotope effect. A ratio k_2/k_1 of (0.997 ± 0.055) (2σ) is obtained from a fit constrained to pass through the origin (Figure 6); a linear fit not forced through the origin gives $k_2/k_1 = 0.98 \pm 0.04$. The accuracy of the relative rate measurements are typically about 5%. The ratio of the absolute rate coefficients at 295 K, $k_2/k_1 = 0.83 \pm 0.13$, suggests a larger kinetic isotope effect, but the uncertainty is considerably larger than for the relative rate determination. An expected k_2/k_1 ratio can be estimated by comparison with related systems; the kinetic isotope effect for Cl + ethane is $k_{C_2H_6}/k_{C_2D_6} = 2.9$,[37,38] and that for the methyl group in CH_3CH_2Cl is $k_{\mathbf{CH_3}CH_2Cl}/k_{\mathbf{CD_3}CH_2Cl} = 6.2$.[39] It seems unlikely that the isotope effect for abstraction from the methyl group in Cl + ethanol would be far outside the range of that observed in these analogous reactions. Given that the fraction that reacts at the methyl site in the Cl + ethanol reaction is 0.07−0.08, assuming a similar kinetic isotope effect for the CH_3 group in CH_3CH_2OH would imply a rate coefficient ratio of k_2/k_1 between 0.93 and 0.95, just within the error bars of both present determinations. The precision of the present measurements is simply inadequate to resolve the kinetic isotope effect of such a minor channel.

Production of vibrationally excited HCl from reactions 1 and 2 can be explained by a direct abstraction mechanism for the Cl + ethanol reaction. Significant vibrational excitation, suggesting a direct reaction where the H−Cl distance in the transition state larger than the equilibrium HCl bond length, has been observed in the exothermic reactions of Cl with propene, allene, and propyne.[23,24] The observation of vibrationally excited product also provides some constraint on the thermochemistry of the reaction. A qualitative upper limit for the vibrational branching is provided by assuming that every reactive collision that has sufficient energy to produce HCl ($v = 1$) does so. Under this assumption, the observation of $f = 0.19$ at 295 K would indicate that 19% of the Cl + ethanol collisions have sufficient energy to make HCl ($v = 1$), corresponding to an activation energy of ∼1 kcal mol^{-1} for production of vibrationally excited HCl. Since the energy of HCl ($v = 1$) is ∼8.3 kcal mol^{-1}, this would imply an exothermicity for reaction 1a of at least 7.3 kcal mol^{-1}. Using D_{298}(H−Cl) = 103.15 kcal mol^{-1},[25] the observed vibrational excitation suggests an α C−H bond energy of less than 95.9 kcal mol^{-1}. Recent measurements of photoelectron spectra of the CH_3CHOH radical by Dyke et al. yield D_{298}(H−$CH(CH_3)$-OH) = 94.5 ± 0.9 kcal mol^{-1},[40] which agrees with the value of 95.2 kcal mol^{-1} derived from ab initio calculations[41] and the 92.6 kcal mol^{-1} lower limit of Ruscic and Berkowitz.[42] No HCl ($v = 1$) is seen in reaction 3. Production of HCl ($v = 1$) from β-hydrogen abstraction is expected to be significantly endothermic, on the basis of the C−H bond energy estimated

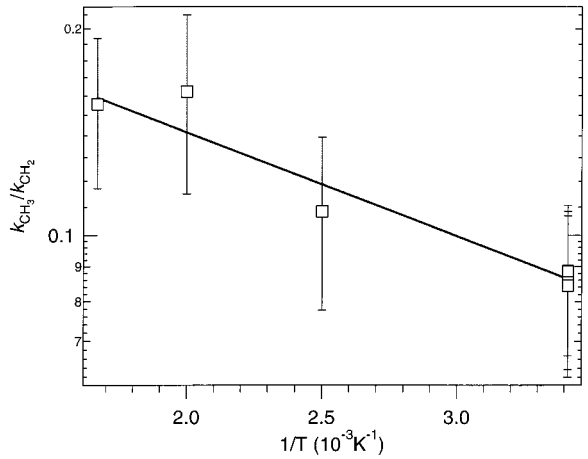

Figure 10. Ratio of β C−H abstraction (k_{CH_3}) to α C−H abstraction (k_{CH_2}) in the Cl + ethanol reaction, deduced from infrared absorption measurements of absolute rate coefficients and HCl yields, shown as a function of temperature. The error bars are $\pm 2\sigma$ based on the accuracy of the individual determinations. The solid line is an Arrhenius fit to the ratio, weighted by the uncertainties, which gives $k_{CH_3}/k_{CH_2} = (0.28 \pm 0.12)e^{-(350 \pm 160)/T}$.

from photoionization mass spectrometry, $D_{298}(H-CH_2CH_2OH) = 99.5$ kcal mol^{-1},[42] and the G2 calculated value of 102.3 kcal mol^{-1}. A recent experimental determination of the CH_2CH_2-OH heat of formation using the equilibrium OH + $C_2H_4 \leftrightarrow CH_2CH_2OH$ at high pressure gives $\Delta H°_{f,0}(CH_2CH_2OH) = -7.4$ kcal mol^{-1},[43] which would correspond to a C−H bond energy in ethanol of $D_{298}(H-CH_2CH_2OH) = 97.4$ kcal mol^{-1}. The product vibrational energy disposal in Cl + ethanol is therefore completely consistent with the previously reported thermochemistry of the reaction.

The site specificity of chlorine atom reactions with hydrocarbons depends mildly on the thermochemistry of the reactions, since barriers to abstraction are small and the H−Cl bond energy is not very different from the C−H bond being broken. The reactions of Cl atoms with propane and butane slightly favor abstraction of a secondary or tertiary hydrogen.[22] While F atoms preferentially abstract the O−H hydrogen in reactions with alcohols, this pathway is endothermic for Cl atoms and is not observed.[1,2,6] The Cl + ethanol reaction has been reported to react almost exclusively (>95%) at the $-CH_2-$ group, on the basis of mass spectroscopic investigations of selectively deuterated ethanols.[7,8] The present results are in qualitative agreement with the mass spectroscopic upper limit but provide a more precise determination of the β-hydrogen abstraction, k_{CH_3}. The β-abstraction fractions determined by the infrared absorption (0.08 ± 0.02) and smog chamber (0.07 ± 0.02) methods at room temperature are in excellent agreement. If the preference for α-hydrogen abstraction is related to its larger exothermicity, the selectivity of the Cl + ethanol reaction should decrease with increasing temperature. Figure 10 shows the ratio of β- to α-hydrogen abstraction derived from the present measurements as a function of temperature. As discussed above, contributions of OH abstraction can be neglected; the ratio k_{CH_3}/k_{CH_2} is then simply $(\phi_3 k_3/k_1)/(1 - \phi_3 k_3/k_1)$. The fraction of β-hydrogen abstraction increases only slightly with temperature, with an Arrhenius fit to the k_{CH_3}/k_{CH_2} ratio yielding $k_{CH_3}/k_{CH_2} = (0.28 \pm 0.12)e^{-(350 \pm 160)/T}$ (the 2σ error bars reflect the precision of the fit). The Cl + ethanol reaction has been used as a CH_3-CHOH source in reactive studies.[7,9] The present results establish the dominance of α-hydrogen abstraction over a wider temperature range and provide a basis for assessment for the share of CH_2CH_2OH produced at elevated temperatures in such experiments.

Conclusions

The reaction of Cl atoms with ethanol has been studied by time-resolved infrared absorption and by smog chamber methods. The reaction proceeds predominantly by α-abstraction to produce $CH_3CH(\bullet)OH$. Vibrational excitation is observed in the HCl product of the α-abstraction, suggesting a C−H bond energy of less than 96 kcal mol^{-1}. The fraction of β-abstraction at 296 K is 0.08 ± 0.02 and increases to 0.14 ± 0.05 at 600 K.

Acknowledgment. We gratefully acknowledge Dr. Thomas Kulp and Dr. Scott Bisson for loan of the diode laser difference-frequency source. The infrared absorption experiments depended on the expert technical assistance of Leonard Jusinski. This work is supported by the Division of Chemical Sciences, the Office of Basic Energy Sciences, the U.S. Department of Energy.

References and Notes

(1) Payne, W. A.; Brunning, J.; Mitchell, M. B.; Stief, L. J. *Int. J. Chem. Kinet.* **1988**, *20*, 63.
(2) Meier, U.; Grotheer, H. H.; Just, T. *Chem. Phys. Lett.* **1984**, *106*, 97.
(3) Nelson, L.; Rattigan, O.; Neavyn, R.; Sidebottom, H.; Treacy, J.; Nielsen, O. J. *Int. J. Chem. Kinet.* **1990**, *22*, 1111.
(4) Wallington, T. J.; Skewes, L. M.; Siegl, W. O.; Wu, C.-H.; Japar, S. M. *Int. J. Chem. Kinet.* **1988**, *20*, 867.
(5) Edelbuttel-Einhaus, J.; Hoyermann, K.; Rohde, G.; Seeba, J. *Proc. Symp. (Int.) Combust.* **1992**, *24*, 661.
(6) Khatoon, T.; Edelbuttel-Einhaus, J.; Hoyermann, K.; Wagner, H. G. *Ber. Bunsen-Ges. Phys. Chem.* **1989**, *93*, 626.
(7) Grotheer, H.-H.; Riekert, G.; Walter, D.; Just, T. *Proc. Symp. (Int.) Combust.* **1988**, *22*, 963.
(8) Meier, U.; Grotheer, H. H.; Riekert, G.; Just, T. *Chem. Phys. Lett.* **1985**, *115*, 221.
(9) Grotheer, H.-H.; Riekert, G.; Walter, D.; Just, T. *Chem. Phys. Lett.* **1988**, *148*, 963.
(10) Pilgrim, J. S.; Taatjes, C. A. *J. Phys. Chem. A* **1997**, *101*, 4172.
(11) Pilgrim, J. S.; Taatjes, C. A. *J. Phys. Chem. A* **1997**, *101*, 8741.
(12) Pilgrim, J. S.; McIlroy, A.; Taatjes, C. A. *J. Phys. Chem. A* **1997**, *101*, 1873.
(13) Balakrishnan, A.; Sanders, S.; DeMars, S.; Webjörn, J.; Nam, D. W.; Lang, R. J.; Mehuys, D. G.; Waarts, R. G.; Welch, D. F. *Opt. Lett.* **1996**, *21*, 952.
(14) Sanders, S.; Lang, R. J.; Myers, L. E.; Fejer, M. M.; Byer, R. L. *Electron. Lett.* **1996**, *32*, 218.
(15) Trutna, W. R.; Byer, R. L. *Appl. Opt.* **1980**, *19*, 301.
(16) Herriott, D.; Kogelnik, H.; Kompfner, R. *Appl. Opt.* **1964**, *3*, 523.
(17) Pilgrim, J. S.; Jennings, R. T.; Taatjes, C. A. *Rev. Sci. Instrum.* **1997**, *68*, 1875.
(18) Tyndall, G. S.; Orlando, J. J.; Kegley-Owen, C. S. *J. Chem. Soc., Faraday Trans.* **1995**, *91*, 3055.
(19) Harrison, A. J.; Cederholm, B. J.; Terwilliger, M. A. *J. Chem. Phys.* **1959**, *30*, 355.
(20) Salahub, D. R.; Sandorfy, C. *Chem. Phys. Lett.* **1971**, *9*, 71.
(21) Satyapal, S.; Park, J.; Bersohn, R.; Katz, B. *J. Chem. Phys.* **1989**, *91*, 6873.
(22) Tyndall, G. S.; Orlando, J. J.; Wallington, T. J.; Dill, M.; Kaiser, E. W. *Int. J. Chem. Kinet.* **1997**, *29*, 43.
(23) Pilgrim, J. S.; Taatjes, C. A. *J. Phys. Chem. A* **1997**, *101*, 5776.
(24) Farrell, J. T.; Taatjes, C. A. *J. Phys. Chem. A* **1998**, *102*, 4846.
(25) Berkowitz, J.; Ellison, G. B.; Gutman, D. *J. Phys. Chem.* **1994**, *98*, 2744.
(26) Leone, S. R. *J. Phys. Chem. Ref. Data* **1982**, *11*, 953.
(27) Wallington, T. J.; Japar, S. M. *J. Atmos. Chem.* **1989**, 399.
(28) Tschuikow-Roux, E.; Niedzielski, J. *J. Photochem.* **1984**, *27*, 141.
(29) Droege, A. T.; Tully, F. P. *J. Phys. Chem.* **1986**, *90*, 1949.
(30) Arunan, E.; Rengarajan, R.; Setser, D. W. *Can. J. Chem.* **1994**, *72*, 568.
(31) Atkinson, R.; Baulch, D. L.; Cox, R. A.; Hampson, R. F., Jr.; Kerr, J. A.; Rossi, M. J.; Troe, J. *J. Phys. Chem. Ref. Data* **1997**, *26*, 521; *J. Phys. Chem. Ref. Data* **1999**, *28*, 191.
(32) Tyndall, G. S.; Wallington, T. J.; Hurley, M. D.; Scheider, W. F. *J. Phys. Chem.* **1993**, *97*, 1576.

(33) Wallington, T. J.; Schneider, W. F.; Nelsen, W.; Barnes, I.; Becker, K. H.; Sehested, J.; Nielsen, O. J. *J. Phys. Chem. A*, in press.
(34) Stein, S. E.; Rukkers, J. M.; Brown, R. L. *NIST Structure & properties database, Ver. 1.2*; NIST: Gaithersburg, MD, 1991.
(35) Wallington, T. J.; Andino, J. M.; Japar, S. M. *Chem. Phys. Lett.* **1990**, *165*, 189.
(36) Niedzielski, J.; Tschuikow-Roux, E.; Yano, T. *Int. J. Chem. Kinet*. **1984**, *16*, 621.
(37) Dobis, O.; Benson, S. W.; Mitchell, T. J. *J. Phys. Chem.* **1994**, *98*, 8, 12264.
(38) Wallington, T. J.; Hurley, M. D. *Chem. Phys. Lett.* **1992**, *194*, 309.
(39) Tschuikow-Roux, E.; Niedzielski, J.; Faraji, F. *Can. J. Chem.* **1985**, *63*, 1093.
(40) Dyke, J. M.; Groves, A. P.; Lee, E. P. F.; Niavaran, M. H. Z. *J. Phys. Chem. A* **1997**, *101*, 373.
(41) Curtiss, L. A.; Lucas, D. J.; Pople, J. A. *J. Chem. Phys.* **1995**, *102*, 3292.
(42) Ruscic, B.; Berkowitz, J. *J. Chem. Phys.* **1994**, *101*, 10936.
(43) Fulle, D.; Hamann, H. F.; Hippler, H.; Jänsch, C. P. *Ber. Bunsen-Ges. Phys. Chem.* **1997**, *101*, 1433.